INTERNATIONAL JOURNAL OF MICROWAVE AND OPTICAL TECHNOLOGY,
VOL.16, NO.1, JANUARY 2021

A Compact Triple Band Notch Reconfigurable Antenna for UWB Applications

Ahmed Samir[1,3], Ahmed Magdy[2], Ebtsam omar[3], Hala M. Abd El Kader[3] and, Ahmed Fawzy[4*]

[1]Department of Communications Engineering, Faculty of Engineering, MTI University, Cairo, Egypt
[2]Electrical Engineering Department, Faculty of Engineering,Suez Canal University, Ismaillia, Egypt
[3]Electrical Engineering Department, Faculty of Engineering (Shoubra), Banha University, Egypt
[4]Nanotechnology Central Lab, Electronics Reasearch Institute, El Tahrir St., Giza, Egypt

E-mail:afawzy@eri.sci.eg

Abstract- **In this paper, a novel design for compact frequency reconfigurable triple slot antenna based on rejected triple band stop functions is demonstrated. An Ultra-Wide Band (UWB) antenna is designed to operate from 3.3 to 12 GHz and printed on a (30 mm × 35 mm) FR4 substrate with permittivity of 4.4 and a thickness of 1.6 mm and also printed on a Rogers4003C substrate with permittivity of 3.38 and a thickness of 1.524 mm. The antenna comprises an inverted double U-slot and an H-Slot on a metallic patch and U-Slot in the feedline to exhibit a triple band-notch functions for the WiMAX band (3.2-3.7 GHz), WLAN-band (5.2-6.3 GHz) and C-band (9-10.8 GHz). To generate a reconfigurable band-stop antenna, the multi Strips (0.4mm×0.5 mm) within the embedded structures are used in the patch plane and feedline. By changing the ON/OFF conditions of the Strips, the antenna can operate in single, dual, and triple-band mode. HFSS simulator program is used to design and simulate results for the proposed antenna. The simulated bandwidth with return loss < -10 dB is (3-12) GHz. The proposed antenna is fabricated and measured. The Simulated and experimental results are compared and found to be in good agreement.**

Index Terms- Ultra wideband(UWB) antenna, U-shaped slot, Frequency-band reconfigurable, Triple notch

I. INTRODUCTION

Recently, the rapid development in wireless communication systems created enormous demands for ultra-wideband antennas to provide very large bandwidth covering several frequency ranges and high gain. The Federal Communications Commission (FCC) released the Ultra-Wide Band (UWB) technology in 2002 for indoor wireless communications, the frequency ranges of (3– 10.6) GHz with maximum radiated power -40 dBm /MHz, and data rate between 100-200 Mbps within 10 m distance [1,2]. The UWB communication systems cover wide bandwidth that overlaps with existing narrowband communications applications, such as WLAN, WiMAX, C-band. Recently, many researchers focus on designing the UWB antenna with band rejection characteristics to eliminate any interference from narrowband wireless applications [3-6]. Many of UWB antennas have been achieved by adding slots with different shapes to produce one or two notched bands by using various technologies [7-10]. The term reconfigurable antenna was introduced in 1998[11]. A reconfigurable antenna extends the capabilities of a conventional antenna by offering the ability to change its configuration, that is to say, to change one or more of its fundamental characteristics by an electrical, mechanical, or other means, according to the needs and environmental context. The antenna is reconfigured by modifying the distribution of the electric current, and consequently the properties of the electromagnetic field and the impedance, and therefore the transmission and reception properties, discretely or continuous manner[12]. There is a very wide variety of reconfigurable antennas and therefore several ways to classify them. This categorization can be done according to the physical property which makes them reconfigurable, the type of reconfigurable components used PIN diodes, varactors diodes, transistors and MEMS switches[13]. Different configurations of this slot have been introduced for this purpose such as U-shaped slot[14], C-shaped slot[15], spoon-shaped slot[16], V-shaped slot[17], triangular-shaped slot[18], T-shaped slot[19], L-shaped slot[20], square-shaped slot[21] and circular-shaped slot [22,23]. Another way of classifying them is to distinguish them according to the configurability functions they offer: reconfiguration in frequency

[24,25]; reconfiguration of radiation [26,27]; reconfiguration of polarization [28,29]; and any combination of the above three configurations. In this paper, A novel UWB antenna design is proposed with three notched bands according to separate the WiMAX band (3.2-3.7 GHz), WLAN-band (5.2-6.3 GHz) and C-band (9-10.8 GHz). The reminder sections are organized as the following. The second section presents the PIN diode characteristics. The proposed antenna design is described in detail in section three. The HFSS simulation results are presented in section four. Overall fabrications and discussion about them are described in section five. Finally, the section six presents the conclusions.

II. PIN DIODE CHARACTRICSTIC AND MODELLING

PIN diodes are widely used as the switching components in different wireless systems. For the reconfigurable antenna, an additional dimension for the RF and the direct current (DC) blocks is required and should be considered in the design of the antenna[30]. The electrical parameters of the PIN diode equivalent model with forward and reverse bias in the ON and OFF state are presented in Fig. 1. The PIN diode is very reliable, high tuning speed, high power-handling, and extremely low cost make it a good choice for the reconfiguration technique [31,32].

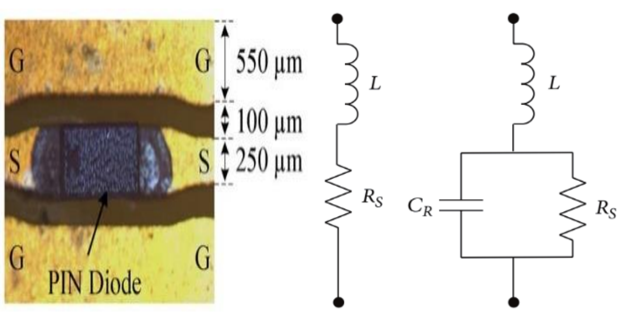

(a) (b) (c)

Fig. 1. (a) Fabricated PIN diode, Equivalent PIN diode model: (b) forward bias (ON state) (c) reverse bias (OFF state).

The HPND-4005 PIN diode is designed for use in strip line or Microstrip circuits and offers exceptional lead strength while achieving excellent electrical performance at high frequencies. We can replace it by making strips through which it is possible to make the antenna also the reconfigurable antenna.

III. ANTENNA STRUCTURE AND DESIGN

The proposed rectangular Microstrip patch antenna is designed on a FR-4 substrate with dielectric constant 4.4 and thickness 1.6 mm. The antenna dimensions are: the substrate width (Ws) = 30 mm and the substrate length (Ls) = 35 mm. The radiation patch has a width (Wp) = 14 mm and length (Lp) = 14.5 mm, the feed line has a width (Wf) = 2.85 mm and length (Lf) = 13.5 mm. The essential parameters for the design of a rectangular Microstrip patch antenna are:

1. Calculation of Patch Width (W)

$$W = \frac{1}{2f_r\sqrt{\mu_0\,\epsilon_0}}\sqrt{\frac{2}{\epsilon r+1}} = \frac{C}{2f_r}\sqrt{\frac{2}{\epsilon r+1}} \quad (1)$$

Where C is the free space velocity of light, ϵr is the dielectric constant of substrate and f_r is the operating frequency.

2. Calculation of Effective Dielectric Constant (Єreff)

$$\epsilon reff = \frac{\epsilon r+1}{2} + \frac{\epsilon r-1}{2}\left[1+12\,\frac{h}{W}\right]^{\frac{-1}{2}} \quad (2)$$

The effective dielectric constant of the rectangular Microstrip patch antenna treats the antenna as if all the fields were contained within a humongous substrate [33].

3. Calculation Extension Length (ΔL)

$$\Delta L = 0.412 \times h \times \frac{(\epsilon eff+0.3)\left(\frac{W}{h}+0.264\right)}{(\epsilon eff-0.258)\left(\frac{W}{h}+0.8\right)} \quad (3)$$

The extension length is used for calculating resonant frequency of Microstrip antenna.

4. Calculation of The Effective Length (Leff) & Actual Patch Length (L)

$$Leff = \frac{1}{2\,f_r\sqrt{\epsilon eff\,\sqrt{\mu_0\,\epsilon_0}}} \quad (4)$$

INTERNATIONAL JOURNAL OF MICROWAVE AND OPTICAL TECHNOLOGY,
VOL.16, NO.1, JANUARY 2021

$$L = Leff - 2\Delta L \tag{5}$$

According to the above equations, Fig. 2. will show the Microstrip patch antenna which can achieve UWB antenna. Fig. 3. appears the parametric study for ground length (Lg) started from 2.5 mm into 35 mm with step equal 2.5 mm to get the optimal ground length which achieved the UWB antenna. We noted that at ground length equal 12.5 mm has UWB started from 3.3 GHz to 10.5 GHz.

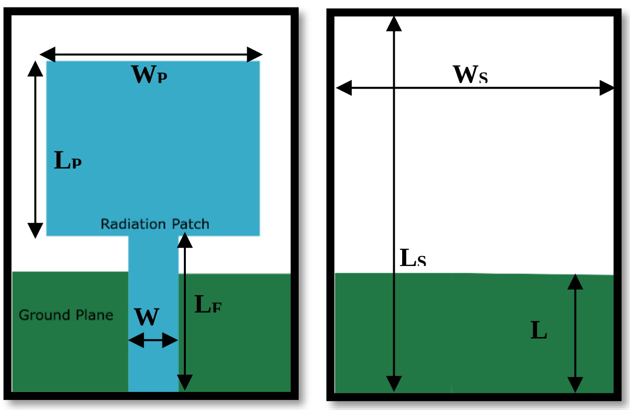

(a) (b)

Fig. 2. Primary Microstrip patch antenna (a) Top view (b) Button view.

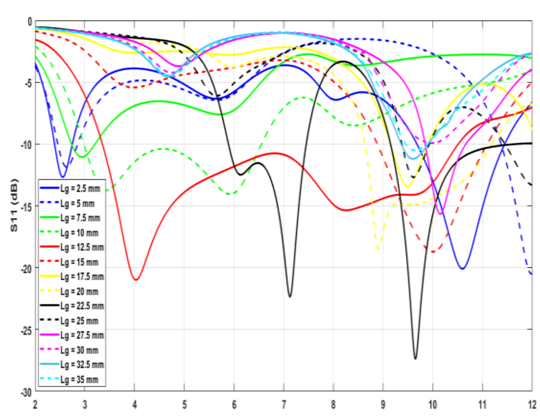

Fig. 3. Optimal ground length using parametric study.

To increase the antenna bandwidth and improve the antenna matching, round steps are added to all corners of the radiation patch by adding slot in the ground plane. Cutting steps in the upper corners of the radiation patch tune the inductive part of the antenna that neutralizes the capacitive coupling between the ground and the patch to get pure resistive input impedance [34,35]. While the slot in the ground plane neutralizes the capacitive effects through the inductive nature of the patch to get nearly pure resistive input impedance [36,37]. as shown in Fig. 4. We can see the result from this change in Fig. 5, where the UWB became wider from 3.3 GHz to 12 GHz.

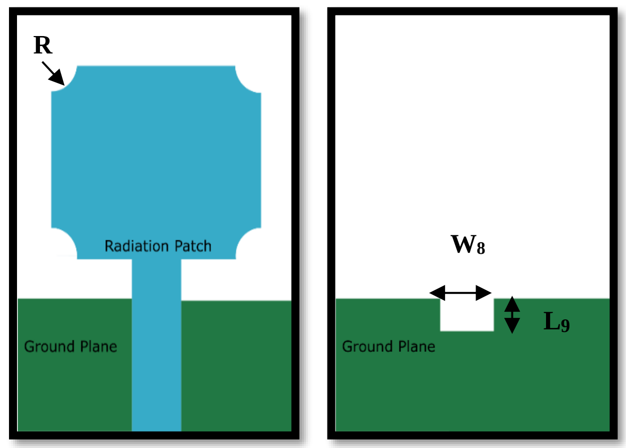

Fig. 4. Modified Microstrip patch antenna.

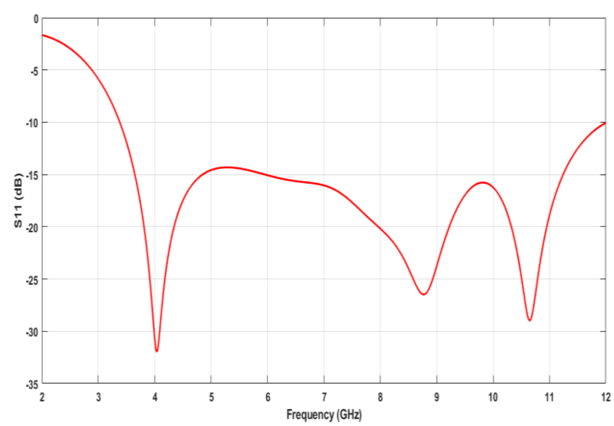

Fig. 5. UWB antenna for modified patch (Return Loss Curve).

As shown in Fig. 6, to achieve band-stop performance at WiMAX and C-Bands, U-Slots have been etched on a metal patch and feedline respectively. The length of U-Slots can be planned with equations (6) and (7). Also, to achieve band-stop performance at WLAN Band, H-Slot has been etched on a metallic patch. The equation (8) for calculation of the width of the H-Slot [38,39].

INTERNATIONAL JOURNAL OF MICROWAVE AND OPTICAL TECHNOLOGY,
VOL.16, NO.1, JANUARY 2021

$$Leq = \{(2 * L_{arm}) + L_{width}\} - (3 * W_{slot}) \quad (6)$$

$$Fr = \frac{C}{2 * Leq * \sqrt{\frac{\epsilon r+1}{2}}} \quad (7)$$

$$W = \frac{(LW - L_s\, W_s)}{L} \quad (8)$$

Where:
Leq: Equivalent length of U-Slot.
Fr: Resonance frequency of notched.
ϵr: Relative permittivity of substrate.

Single stop band, UWB antenna is integrated with WiMAX band-notched inverted U-Slot as shown in Fig. 7 (a). The Fig. 7 (b) shows the return loss in this antenna design to eliminate WIMAX band.

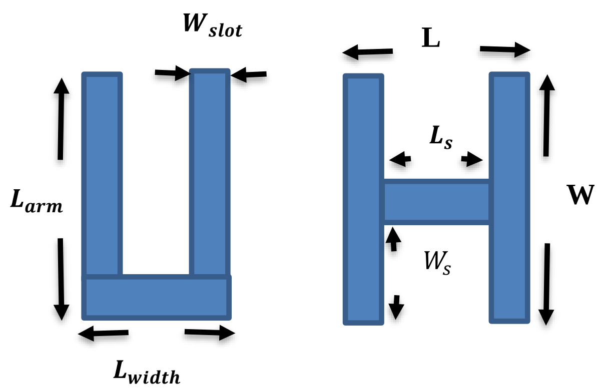

Fig. 6. Band stop slot dimensions (a) U-Slot and (b) H-Slot.

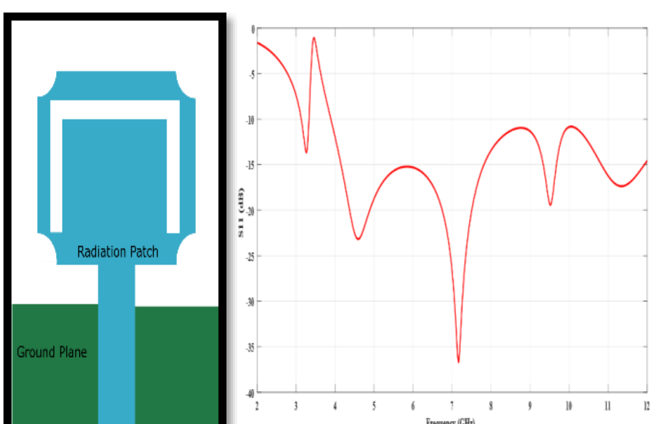

(a) (b)

Fig. 7. Single stop band using Inverted U-slot (a) antenna geometry (b) return loss.

Double stopband, UWB antenna is integrated with WiMAX band-notched inverted U-Slot and WLAN band-notched H-Slot as shown in Fig. 8 (a). The Fig. 8 (b) shows the return loss in this antenna design to eliminate WIMAX band and WLAN band.

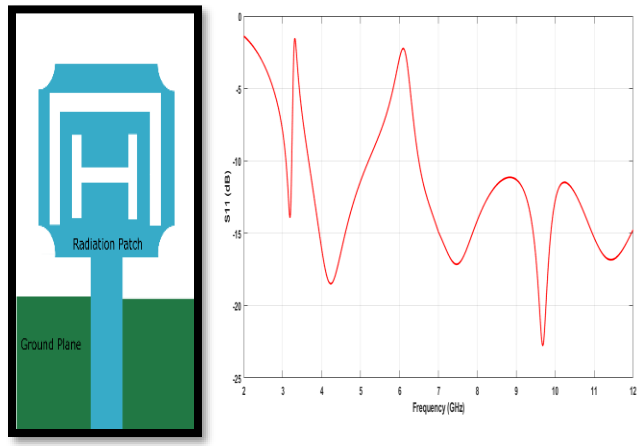

(a) (b)

Fig. 8. Double stop band using Inverted U-slot & H-slot (a) antenna geometry (b) return loss.

Triple stopband, UWB antenna is integrated with WiMAX band-notched inverted U-Slot, WLAN band-notched H-Slot, and U-Slot to produce C-band as shown in fig. 9 (a). The Fig. 9 (b) shows the return loss in this antenna design to eliminate WIMAX band, C-band and WLAN band.

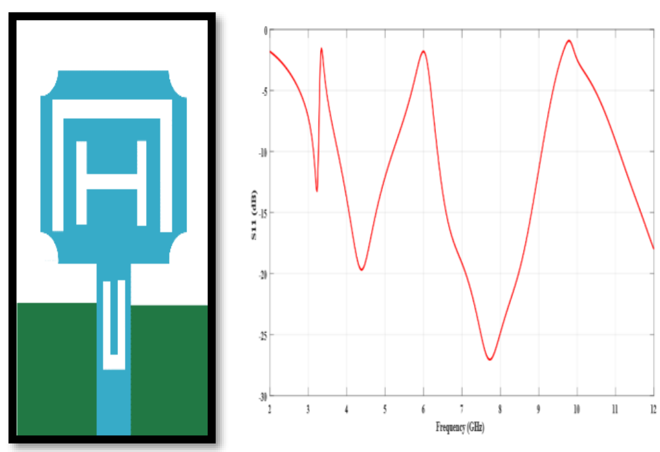

(a) (b)

Fig. 9. Triple stop band using Inverted U-slot, H-slot & U-slot in feedline (a) antenna geometry (b) return loss.

As shown in Fig. 10, the configuration of the multi-slot antenna which consists of a rectangular radiation patch, two slots etched in the patch, and a Microstrip feed line with U slot etched in the feed line. All dimensions of the slots are illustrated in Table 1.

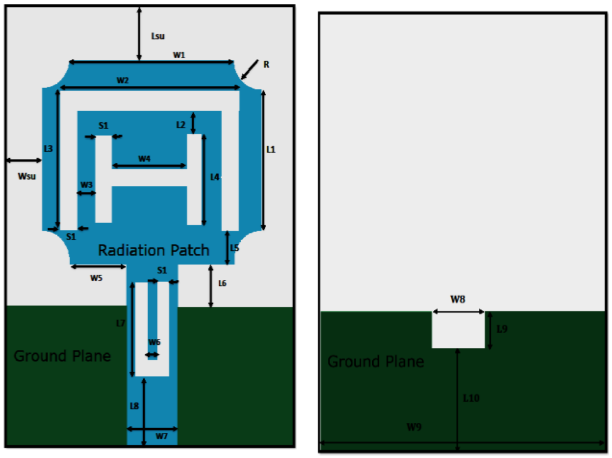

(a) (b)

Fig. 10. Configuration of the proposed antenna.
(a) Top layer (b) Bottom layer

Table 1: Parameters of the proposed antenna (unit: mm)

L1	L2	L3	L4	L5	L6	L7	L8
6.5	1.9	9.95	6.88	2.55	1.5	5.1	6
L9	L10	S1	Lsu	Wsu	R	W1	W2
2	10.5	0.5	7	8	2	10	11.4
W3	W4	W5	W6	W7	W8	W9	H
1.45	6.5	3.58	0.5	2.85	3	30	1.524

IV. SIMULATION RESULTS

Fig. 11 illustrates the five different cases of the antenna design using three strips. The variations of the reflection coefficient (S11) with frequency for these design cases are provided in Fig. 10. The variations of VSWR with frequency for these design cases are provided in Fig. 11. Case-1 shows the triple stop band antenna when no strips are found. Case-2 shows the double stop band antenna when added strip to the U-slot feedline. Case-3 we will add two strips to the U-slot feedline and H-slot patch, here only a single stop band will occur. In Case-4, we will add two strips to the inverted U-slot patch and H-slot patch, here only a single stop band will occur. In the last proposed design Case-5, shows the double stop band antenna when added strip to the H-slot patch. All cases are summarized in Table 2.

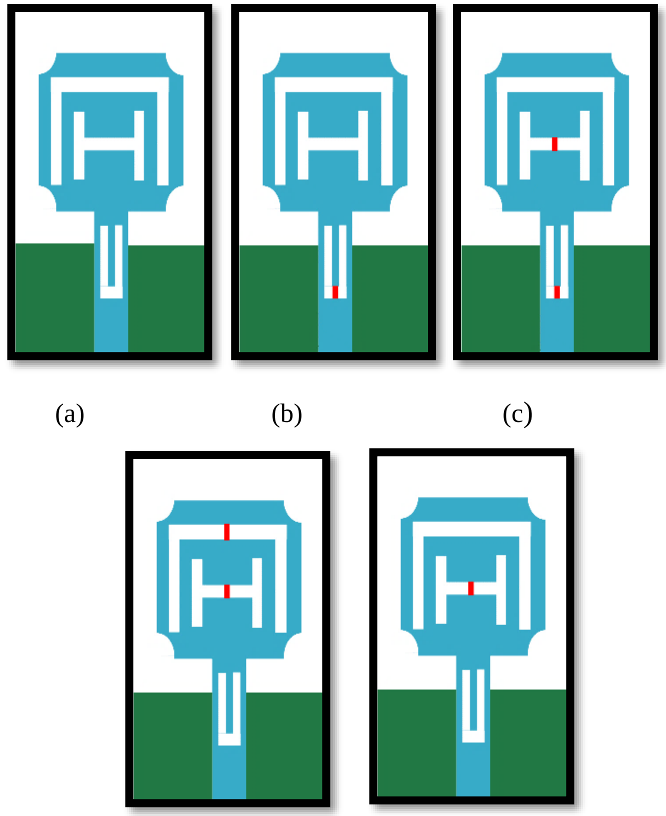

(a) (b) (c)

(d) (e)

Fig. 9. Geometry of proposed antenna at five cases
(a) Case 1 (b) Case 2 (c) Case 3 (d) Case 4 (e) Case 5.

Table 2: Number of stop bands cross ponding to case number

Case Number	Number of Stop Bands
Case 1	Triple Stop Bands (WiMAX, WLAN & C-Band)
Case 2	Double Stop Bands (WiMAX & WLAN)
Case 3	Single Stop Band (WiMAX Only)
Case 4	Single Stop Band (C-Band Only)
Case 5	Double Stop Bands (WiMAX & C-Band)

In Fig. 12, the variations of reflection coefficient with frequency for five cases have a good performance also in Fig. 13, the variations of voltage standing wave ratio for the five cases are the same performance.

INTERNATIONAL JOURNAL OF MICROWAVE AND OPTICAL TECHNOLOGY,
VOL.16, NO.1, JANUARY 2021

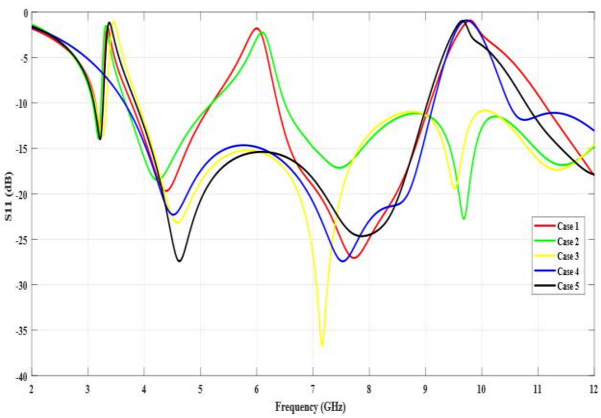

Fig. 12. The variations of Reflection Coefficient (S11) with frequency for design cases.

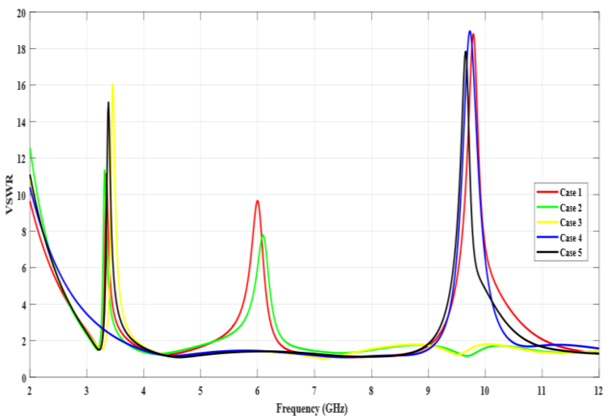

Fig. 13. The variations of Voltage Standing Wave Ratio (VSWR) with frequency for design cases.

The radiation pattern for proposed antenna are presented in Fig. 14, where the E and H planes are the y-z plane (ϕ = 90o and 0o < ϴ <180o) and the x-z plane (ϕ =0o and 0o < ϴ <180o) respectively at 3.3, 6 and 9.8 GHz. Radiation patterns in the E-plane are about the same as shown in Fig. 14 (a)-(c).

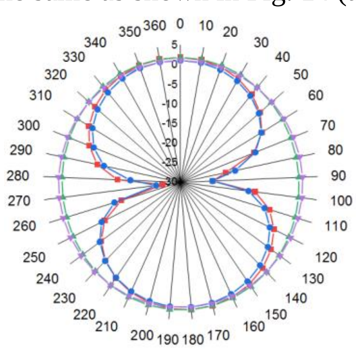

(a)

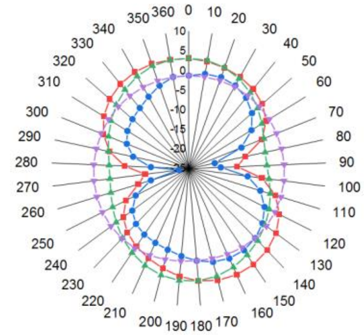

(b)

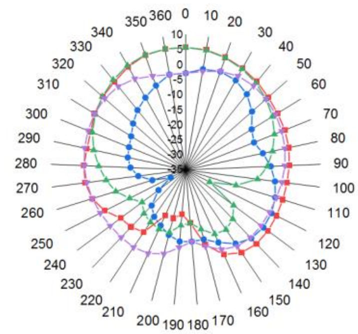

(c)

Fig. 14. Radiation patterns of Rogers4003C antenna in case1 (a) 3.3 GHz (b) 6 GHz (c) 9.8 GHz.

E-Sim E-Meas.

H-Sim H-Meas.

The consequence of current distribution on the proposed antenna at various frequencies is depicted in Fig. 15. At chosen frequencies like 3.3, 6 & 9.8 GHz with are the stopbands, and inconsistent current accumulation is found near the edges of the corresponding slot whereas uniform current distribution for displaying in Fig. 15 (a)-(c).

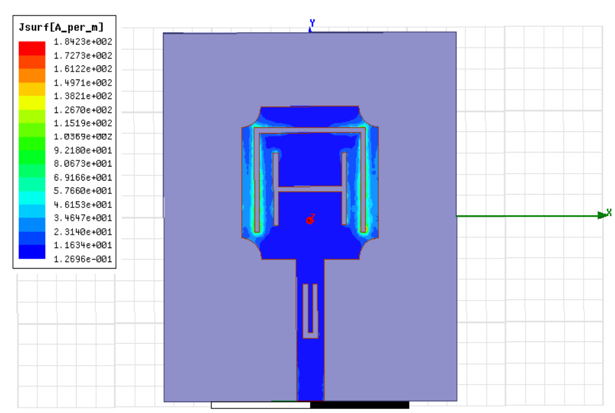

(a)

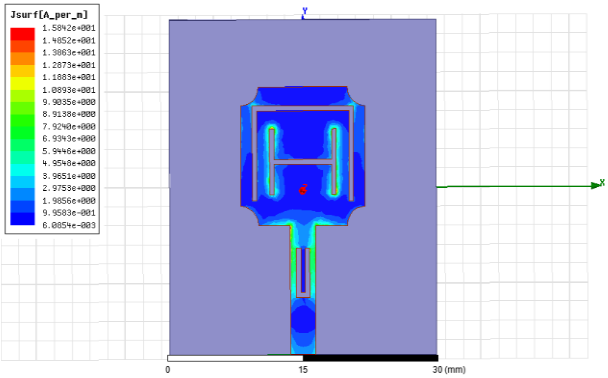

(b)

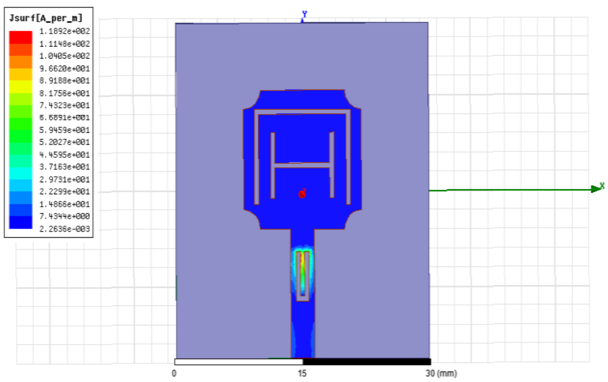

(c)

Fig. 15. Current distribution of Rogers4003C antenna in case1 (a) 3.3 GHz (b) 6 GHz (c) 9.8 GHz.

V. EXPERIMANTEL RESULTS AND DISCUSION

In this section, we will study the effect of the substrate on which the antenna is fabricated. These materials are FR4 and Rogers4003C, each material has advantages and disadvantages. When we discuss FR4 material is cheap and available, but at microwave frequencies is very lossy material. On the other hand, Rogers4003C material has an excellent response at microwave frequencies in the following figure we will show the fabrication design for each material as shown in Fig. 16. From the following results, the rogers4003C material has better performance than FR4 material. When we note the difference between Fig. 18 and Fig. 19 w.r.t reflection coefficient curves, the measured output of the FR4 material near the simulated output until 5GHz after that we found a big different between the two curves but at Rogers4003C material, the two curves are very closed. We consider that Rogers4003C is very suitable for UWB antenna design which covered frequencies until 12 GHz.

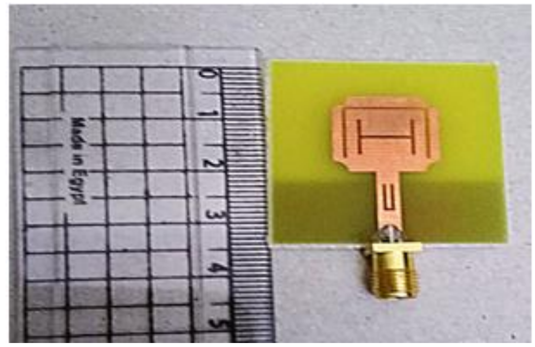

(a)

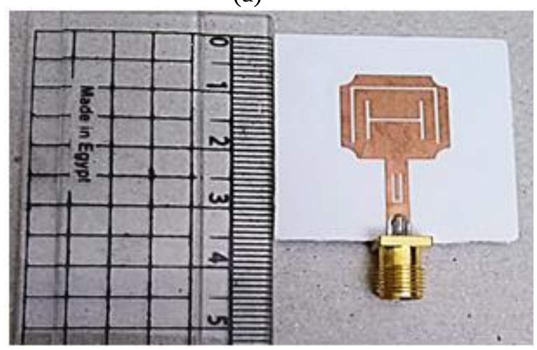

(b)

Fig. 16. Fabricated antenna prototype (a) FR4 antenna (b) Rogers4003C antenna.

In Fig. 17, we can observe the measured reflection coefficient (S11) in case 1 for both antennas FR4 antenna and Rogers4003c antenna by using ZVB 20 Vector Network Analyzer.

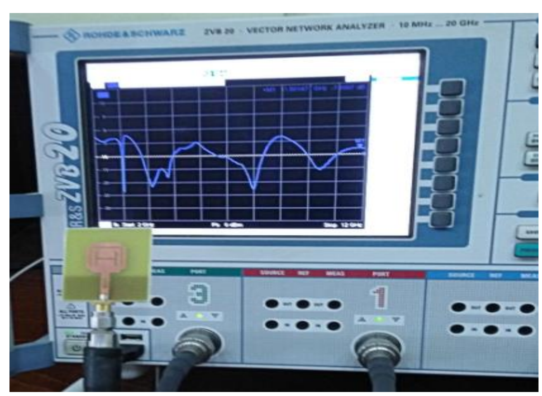

(a)

INTERNATIONAL JOURNAL OF MICROWAVE AND OPTICAL TECHNOLOGY,
VOL.16, NO.1, JANUARY 2021

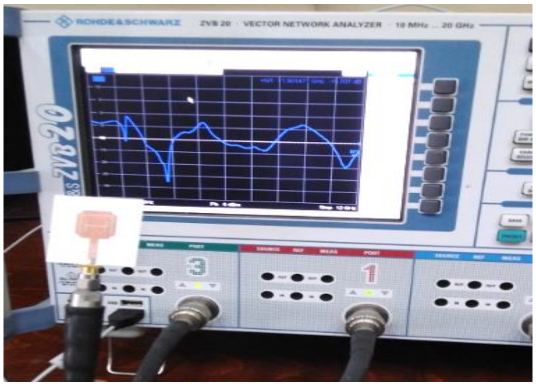

(b)

Fig. 17. Measured Reflection Coefficient (S11) using ZVB 20 Vector Network Analyzer in case 1(a) FR4 antenna (b) Rogers4003C antenna.

In Fig. 18, the difference between the reflection coefficient curves of simulated and measured of FR4 antenna in case 1 is very clear, which forces us not to resort to this material, especially at high frequencies, because we will get unsatisfactory results compared to the results we obtained when using rogers4003c material. The fabricated FR4 antenna has frequency band of 3.02 to over 11GHz with three rejection bands around 3.08-3.82, 5.01-6.65 and 8.36-9.95 GHz with respect to the simulated FR4 antenna has frequency 2.81 to over 12 GHz with three rejection bands around 3-3.39, 4.98-5.98 and 7.92-9.46 GHz.

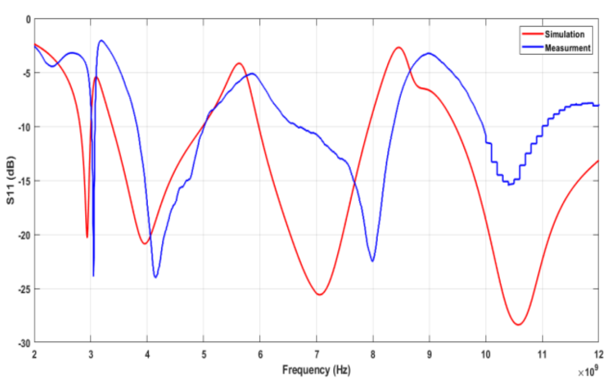

Fig. 18. Simulated and Measured reflection coefficient of FR4 antenna in case 1.

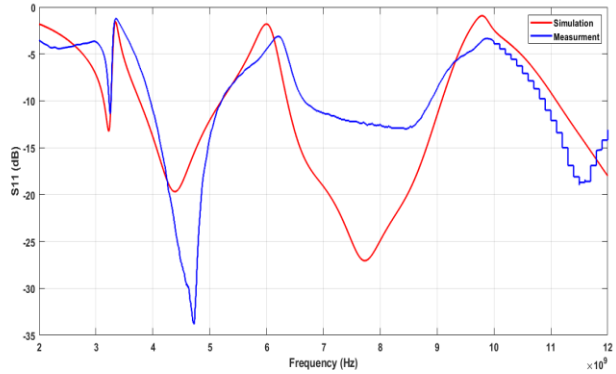

Fig. 19. Simulated and Measured reflection coefficient of Rogers4003C antenna in case 1.

In Fig. 19, which shows the extent of the strong convergence between the reflection coefficient curves of simulated and measured of Rogers4003c antenna in all three stop bands. The fabricated Rogers4003c antenna has frequency band of 3.23 to over 12 GHz with three rejection bands around 3.23-3.96, 5.21-6.66 and 8.88-10.9 GHz with respect to the simulated Rogers4003c antenna has frequency 3.14 to over 12 GHz with three rejection bands around 3.26-3.377, 5.2-6.37 and 9.08-11.1GHz. A discrepancy between the measured data and the simulated results exists, which could be due to the effect of the SMA port. By carefully performing the manufacturing and measurement process more accurate results can be obtained.

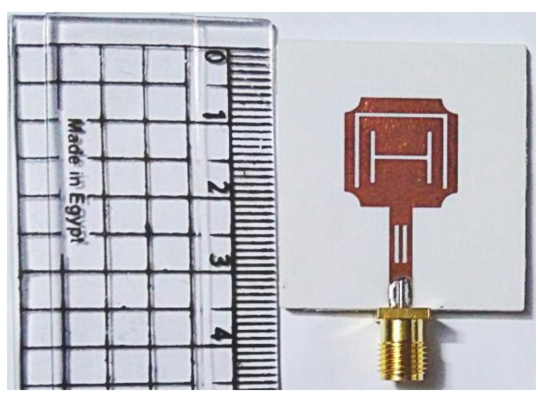

(a)

IJMOT
INTERNATIONAL JOURNAL OF MICROWAVE AND OPTICAL TECHNOLOGY,
VOL.16, NO.1, JANUARY 2021

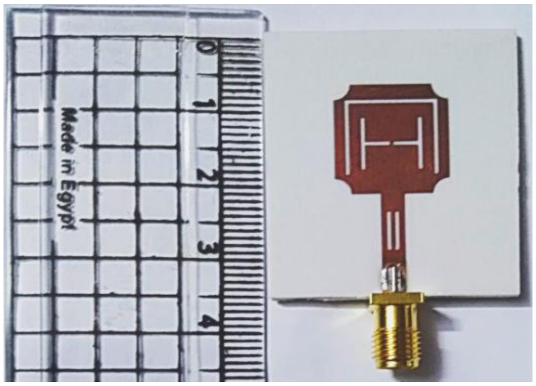

(b)

Fig. 20. Fabricated Rogers4003C antenna prototype (a) Case 2 (b) Case 3.

In Fig. 20, we have the second and third cases, and as it appears in Rogers4003c antenna manufacturing, in the case 2 we make the double band rejection of the first band (WiMAX-Band) and the second band (WLAN-Band), and this is done by adding the strip to the U-shaped slot in feedline and also in the case 3 we make the single band rejection of the first band (WLAN-Band) only, and this is done by adding the strips to H-shaped slot in radiating patch and the U-shaped slot in feedline together.

In Fig. 21, which shows the extent of the strong convergence between the reflection coefficient curves of simulated and measured of Rogers4003c antenna in case 2. The fabricated Rogers4003c antenna in case 2 has double rejection bands around 3.25-3.87 and 5.45-6.48 GHz with respect to the simulated Rogers4003c antenna has double rejection bands around 3.23-3.367and 5.2-6.5GHz.

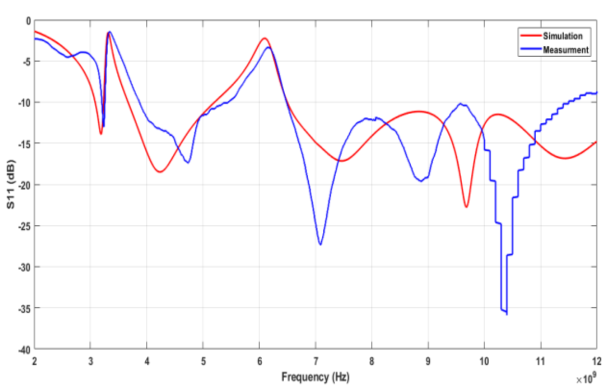

Fig. 21. Simulated and Measured reflection coefficient of Rogers4003C antenna in case 2.

In Fig. 22, which shows the extent of the strong convergence between the reflection coefficient curves of simulated and measured of Rogers4003c antenna in case 3. The fabricated Rogers4003c antenna in case 3 has single rejection band around 3.31-4.09 GHz with respect to the simulated Rogers4003c antenna has single rejection band around 3.32-3.89GHz.

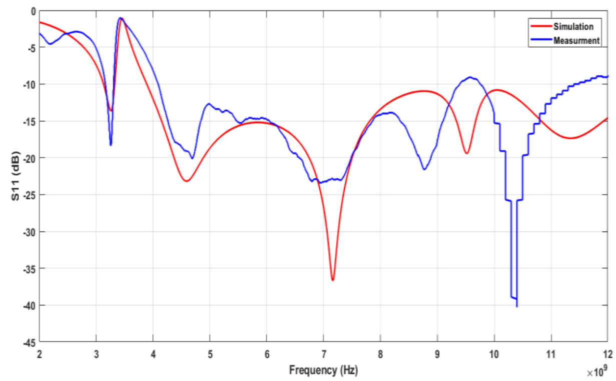

Fig. 22. Simulated and Measured reflection coefficient of Rogers4003C antenna in case 3.

In Table 3, we will review a comparison between more than antenna design in terms of several parameters such as substrate size, relative permittivity of substrate, number of notch, band notch gains and frequency band.

INTERNATIONAL JOURNAL OF MICROWAVE AND OPTICAL TECHNOLOGY,
VOL.16, NO.1, JANUARY 2021

Table 3: Comparison of proposed antenna with recently presented antennas

Ref []	Size (mm^3)	ε_r	No. of Notched	Band Notch Gain (dBi)	Frequency Band (GHz)
Sarkar,[40]	35×35×1.6	4.4	3 (WiMAX, WLAN, X-Band)	-5, -1,-3	2.21 – 12.83
Wang,[41]	30×30×1.6	4.4	3 (WiMAX, WLAN, ITU Band)	1, 1.5,1	3 – 12
Yadav,[42]	26×30×1.6	4.4	3 (WiMAX, WLAN, X-Band)	-5,-5,-0.5	3 – 11
Srivastava, [43]	30×35×1.6	4.4	3 (WiMAX, WLAN, X-Band)	-2,-2, -3	2.8 – 11.42
Yadav,[44]	26×30×1.6	4.4	3 (WiMAX-Band, WLAN)	-2.8, -3.5, -1.5	3 – 11
Present Work	30×35×1.524	3.38	3 (WiMAX, WLAN, C-Band)	-2.3, -0.7, -1.3	3.3 – 12

VI. CONCLUSIONS

In this paper, a UWB Antenna with Triple Reconfigurable Notched Rejection Bands was presented. The simulation results of the reflection coefficients (S11) and voltage standing wave ratio (VSWR) demonstrated that the antenna has an ultra-wideband which covers the frequency range of 3.0 to 12 GHz. By embedding an inverted U-slot in the radiating patch, a frequency band notch was between the bandwidth (3.2-3.7 GHz) for WiMAX application. H-slot in the radiating patch, a frequency band notch was between the bandwidth (5.2-6.3 GHz) for WLAN application. U-slot in the feedline, a frequency band notch was between the bandwidth (9-10.8 GHz) for C-Band application. According to the proposed simulations and fabrications for a novel antenna design, the proposed antenna could be a good candidate for the reconfigurable notched rejection UWB antenna.

REFERENCES

[1] N. M. Awad and M. K. Abdelazeez, "Multislot Microstrip antenna for ultra-wide band applications," *Journal of King Saud University - Engineering Sciences*, Vol. 30, No. 1, pp. 38–45, December 2018.

[2] Wang, R., L.-J. Zhang, and S.-W. Hu, "A novel ACPW-fed quad-band hybrid antenna for wireless applications," *International Journal of Microwave and Wireless Technologies*, Vol. 10, No. 4, pp. 460-468, January 2018.

[3] N. Ojaroudi, Y. Ojaroudi, S. Ojaroudi, Y. Ebazadeh, and M. Shirgir, "Small Reconfigurable Monopole Antenna Integrated with PIN Diodes for Multimode Wireless Communications," *ACES Journal*, Vol. 29, No. 7, pp. 541–546, July 2014.

[4] N. O. Parchin, H. J. Basherlou, Y. I. A. Al-Yasir, A. M. Abdulkhaleq, and R. A. Abd-Alhameed, "Reconfigurable antennas: Switching techniques— a survey," *Electronics (Switzerland)*, Vol. 9, No. 2, February 2020.

[5] Pozar, D. M., "Microstrip antennas," *Proceedings of the IEEE*, Vol.80, No. 1, pp. 79-91, 1992.

[6] Mansoul, F. Ghanem, M. R. Hamid, E. Salonen, and M. Berg, "Bandwidth reconfigurable antenna with a fixed lower and a variable upper limit," *IET Microwaves, Antennas Propag.*, Vol. 10, No. 15, pp. 1725–1733, December 2016.

[7] D. Rodrigo, B. A. Cetiner, and L. Jofre, "Frequency, radiation pattern and polarization reconfigurable antenna

using a parasitic pixel layer," *IEEE Trans. Antennas Propag.*, Vol. 62, No. 6, pp. 3422–3427, June 2014.

[8] Y. Y. Bai, S. Xiao, M. C. Tang, C. Liu, and B. Z. Wang, "Pattern reconfigurable antenna with wide angle coverage," *Electron. Lett.*, Vol. 47, No. 21, pp. 1163–1164, October 2011.

[9] D. H. Lee and S. Pyo, "Dual-reconfigurable Microstrip antenna for polarization agility and diversity," *Electron. Lett.*, Vol. 51, No. 16, pp. 1226–1227, August 2015.

[10] P. Zhang, S. Liu, R. Chen, and X. Huang, "A reconfigurable Microstrip patch antenna with frequency and circular polarization diversities," *Chinese J. Electron.*, Vol. 25, No. 2, pp. 379–383, August 2016.

[11] Balanis, C. A., Theory Analysis and Design, 4th edition, *John Wiley & Sons*, 2016.

[12] G. Srivastava, S. Dwari, and B. K. Kanaujia, "A compact triple band notch circular ring antenna for UWB applications," *Microw. Opt. Technol. Lett*., Vol. 57, No. 3, pp. 668–672, January 2015.

[13] Y. Li, W. Li, and Q. Ye, "A reconfigurable triple-notch-band antenna integrated with defected Microstrip structure band-stop filter for ultra-wideband cognitive radio applications," *Int. J. Antennas Propag.*, Vol. 2013, June 2013.

[14] H. M. Zamel, A. M. Attiya, and E. A. Hashish, "Design of a Compact UWB Planar Antenna with Band-Notch Characterization," *Radio Science Conference*, March 2007.

[15] O. M. Haraz, "A Compact CPW Fed Ultra-Wideband Antenna with a Band-Notch Characteristic," *IEEE International Conference*, pp. 426-430, November 2012.

[16] Mohamed, I., A. Elhassane, B. Hamid, H. Mostafa, and L. Mohamed, "Design of compact tri-band fractal antenna for RFID readers," *International Journal of Electrical and Computer Engineering (IJECE)*, Vol. 7, No. 4, pp. 2036-2044, November 2017.

[17] Y. Kim and D. H. Kwon, "Planar Ultra Wide Band Slot Antenna with Frequency Band Notch Function," *IEEE AP-S Int. Symp*, pp. 1788-1791, June 2004.

[18] Mansoul, F. Ghanem, M. R. Hamid, and M. Trabelsi, "A selective frequency-reconfigurable antenna for cognitive radio applications," *IEEE Antennas Wirel. Propag. Lett.*, Vol. 13, pp. 515–518, March 2014.

[19] N. O. Parchin, H. J. Basherlou, and R. A. Abd-alhameed, "A Design of Crossed Exponentially Tapered Slot Antenna with Multi-Resonance Function for 3G / 4G / 5G Applications," *Prog. Electromagn. Res. Letters*, Vol. 92, pp. 1–8, May 2020.

[20] M. Ojaroudi, N. Ojaroudi, and N. Ghadimi, "UWB Slot Antenna with Band-Stop Operation by Using H-Shaped Parasitic Structures for UWB Applications," *ACES Journal*, Vol. 28, No. 12, pp. 1259–1264, December 2013.

[21] T. Sedghi, M. Jalali, and T. Aribi, "Fabrication of CPW-Fed Fractal Antenna for UWB Applications with Omni-Directional Patterns," *The Scientific World Journal*, Vol. 2014, February 2014.

[22] S. Tomar and A. Kumar, "Design of a Triple Band-notched UWB Planar Monopole Antenna," *J. Microw. Optoelectron. Electromagn. Appl.*, Vol. 14, No. 2, pp. 184–196, December 2015.

[23] G. Gao, L. He, B. Hu, and X. Cong, "Novel dual band-notched UWB antenna with T-shaped slot and CSRR structure," *Microw. Opt. Technol. Lett.*, Vol. 57, No. 7, pp. 1584–1590, October 2015.

[24] Clemente, L. Dussopt, R. Sauleau, P. Potier, and P. Pouliguen, "1-bit reconfigurable unit cell based on PIN diodes for transmit-array applications in X-band," *IEEE Trans. Antennas Propag.*, Vol. 60, No. 5, pp. 2260–2269, March 2012.

[25] B. Mun, C. Jung, M. J. Park, and B. Lee, "A compact frequency-reconfigurable multiband LTE MIMO antenna for laptop applications," *IEEE Antennas Wirel. Propag. Lett.*, Vol. 13, pp. 1389–1392, July 2014.

[26] Yadav, M. D. Sharma, and R. P. Yadav, "A CPW-Fed CSRR and Inverted U Slot Loaded Triple Band Notched UWB Antenna," *Prog. Electromagn. Res. C*, Vol. 89, pp. 221-231, January 2019.

[27] H. Nazeri, A. Falahati, and R. M. Edwards, "A novel compact fractal UWB antenna with triple reconfigurable notch reject bands applications," *AEU - Int. J. Electron. Commun.*, Vol. 101, pp. 1–8, March 2019.

[28] Liu, L. Liu, S. W. Cheung, and T. I. Yuk, "Title Bandwidth improvements using ground slots for compact UWB Microstrip-fed antennas," *Prog. Electromagn. Res .C*, pp. 1420–1423, September 2011.

[29] Rahman, M. and M. A. Stuchly, "Transmission line-periodic circuit representation of planar microwave photonic bandgap structures," *Microw. Opt. Technol. Lett.*, Vol. 30, pp. 15-19, May 2001.

[30] T. Sabapathy, R. B. Ahmad, M. Jusoh, and M. R. Kamarudin, "A Pattern-Reconfigurable Parasitic Patch Antenna Using BAR and HPND PIN Diode,", pp. 2–4, April 2014.

[31] A. S. A. Jabar and D. K. Naji, "Design of Miniaturized Quad-Band Dual-Arm Spiral Patch Antenna for RFID, WLAN and WiMAX Applications," *Prog. Electromagn. Res. C*, Vol. 91, pp. 97-113, March 2019.

[32] M. I. Lai, T. Y. Wu, J. C. Hsieh, C. H. Wang, and S. K. Jeng, "Design of reconfigurable antennas based on an L-shaped slot and PIN diodes for compact wireless devices," *IET Microwaves, Antennas Propag.*, Vol. 3, No. 1, pp. 47–54, January 2009.

[33] Gautam, A. K., L. Kumar, B. K. Kanaujia, and K. Rambabu, "Design of compact F-shaped slot triple-band antenna for WLAN/WiMAX applications," *IEEE Trans. Antennas Propag.*, Vol. 64, No. 3, pp. 1101-1105, December 2016.

[34] G. K. Pandey, H. S. Singh, P. K. Bharti, and M. K. Meshram, "Design and Analysis of Ψ-Shaped UWB Antenna with Dual Band Notched Characteristics," *Wirel. Pers. Commun.*, Vol. 89, No. 1, pp. 79–92, March 2016.

[35] F. Yu and C. Wang, "A CPW-Fed Novel Planar Ultra-Wideband Antenna with a Band-Notch Characteristic," *Radio Engineering*, Vol.18, December 2009.

[36] H. Elftouh, N. A. Touhami, M. Aghoutane, S. El Amrani, A. Tazon, and M. Boussouis, "Miniaturized Microstrip Patch Antenna with Defected Ground Structure," *Prog. Electromagn. Res. C*, Vol. 55, pp. 25-33, November 2014.

[37] C. Arora, S. S. Pattnaik, and R. N. Baral, "Dual band Microstrip patch antenna array loaded with split ring resonators and via holes," *AEU - Int. J. Electron. Commun.*, Vol. 93, June 2017.

[38] M. Ojaroudi, N. Ojaroudi, and N. Ghadimi, "UWB Slot Antenna with Band-Stop Operation by Using H-Shaped Parasitic Structures for UWB Applications," *ACES Journal*, Vol. 28, No. 12, pp. 1259–1264, December 2013.

[39] X. Bao and M. Ammann, "Conference papers Printed band-rejection UWB antenna with H- shaped slot," *Int Workshop Antenna Technol*, pp.10–15, October 2007.

[40] Sarkar, D., K. V. Srivastava, and K. Saurav, “A compact Microstrip-fed triple band-notched UWB monopole antenna,” *IEEE Antennas Wirel. Propag. Lett.*, Vol. 13, pp. 396-399, March 2014.

[41] Wang, Z., J. Liu, and Y. Yin, “Triple band-notched UWB antenna using novel asymmetrical resonators,” *Int. J. Electron. Commun. (AEU),* Vol. 70, No. 12, pp. 1630-1636, December 2016.

[42] Yadav, A., et al., “SRR and S-shape slot loaded triple band notched UWB antenna,” *Int. J. Electron. Commun. (AEU),* Vol. 79, pp. 192-198, September 2017.

[43] Srivastava, G., S. Dwari, and B. K. Kanaujia, “A compact triple band notch circular ring antenna for UWB application,” *Microw. Opt. Technol. Lett.*, Vol. 53, No. 3, pp. 668-672, December 2015.

[44] Yadav, M. D. Sharma, and R. P. Yadav, “A CPW-fed CSRR and inverted u slot loaded triple band notched UWB antenna,” *Prog. Electromagn. Res. C,* Vol. 89, pp. 221–231, January 2019.